Acta Crystallographica Section F
Structural Biology and Crystallization Communications
ISSN 1744-3091

The structure of mAG, a monomeric mutant of the green fluorescent protein Azami-Green, reveals the structural basis of its stable green emission

Tatsuki Ebisawa, Akihiro Yamamura, Yasuhiro Kameda, Kou Hayakawa, Koji Nagata and Masaru Tanokura*

Department of Applied Biological Chemistry, Graduate School of Agricultural and Life Sciences, University of Tokyo, 1-1-1 Yayoi, Bunkyo-ku, Tokyo

Correspondence e-mail: amtanok@mail.ecc.u-tokyo.ac.jp

Received 21 January 2010
Accepted 24 March 2010

PDB Reference: monomeric mutant of Azami-Green, 3adf.

Monomeric Azami-Green (mAG) from the stony coral *Galaxea fascicularis* is the first known monomeric green-emitting fluorescent protein that is not a variant of *Aequorea victoria* green fluorescent protein (avGFP). These two green fluorescent proteins are only 27% identical in their amino-acid sequences. mAG is more similar in its amino-acid sequence to four fluorescent proteins: Dendra2 (a green-to-red irreversibly photoconverting fluorescent protein), Dronpa (a bright-and-dark reversibly photoswitchable fluorescent protein), KikG (a tetrameric green-emitting fluorescent protein) and Kaede (another green-to-red irreversibly photoconverting fluorescent protein). To reveal the structural basis of stable green emission by mAG, the 2.2 Å crystal structure of mAG has been determined and compared with the crystal structures of avGFP, Dronpa, Dendra2, Kaede and KikG. The structural comparison revealed that the chromophore formed by Gln62-Tyr63-Gly64 (QYG) and the fixing of the conformation of the imidazole ring of His193 by hydrogen bonds and van der Waals contacts involving His193, Arg66 and Thr69 are likely to be required for the stable green emission of mAG. The crystal structure of mAG will contribute to the design and development of new monomeric fluorescent proteins with faster maturation, brighter fluorescence, improved photostability, new colours and other preferable properties as alternatives to avGFP and its variants.

1. Introduction

Green fluorescent proteins (GFPs), which were first isolated from the bioluminescent jellyfish *Aequorea victoria* (avGFP; reviewed by Shimomura, 2006), are crucial tools in molecular and cellular biology as translational reporters, fusion tags and biosensors (Tsien, 1998). avGFP adopts a β-can fold (Yang *et al.*, 1996; Ormö *et al.*, 1996) consisting of an 11-stranded β-barrel and a coaxial central α-helix holding a Ser65-Tyr66-Gly67 (SYG) chromophore. Recent studies have enabled the structure-based mutageneses of avGFP and other anthozoan fluorescent proteins to develop derivatives with desirable properties, *e.g.* enhanced green emission, red-shifted fluorescence and photo-inducible green-to-red conversion. All of the anthozoan avGFP-like proteins characterized to date form obligatory oligomers (Zhang *et al.*, 2002) which are not suitable for fluorescence resonance energy-transfer (FRET) experiments (reviewed by Müller-Taubenberger & Anderson, 2007; Shaner *et al.*, 2007). Karasawa *et al.* (2003) cloned the gene of Azami-Green (AG; 27% sequence identity to avGFP), a tetrameric green-emitting fluorescent protein containing the Gln65-Tyr66-Gly67 (QYG) chromophore, from the stony coral *Galaxea fascicularis* and established its monomeric mutant, mAG, by introducing three point mutations: Y123T, Y188A and F190K. mAG is the first known monomeric green-emitting fluorescent protein that is not a variant of avGFP. Thus, mAG is an alternative to avGFP and its variants and can be used as a translational reporter, a fusion tag and a biosensor in FRET experiments.

Despite the usefulness of mAG, the structural basis of its stable green emission has not been identified. To reveal this basis, we have determined the 2.2 Å crystal structure of mAG and compared it with the crystal structures of highly homologous proteins with various fluorescent properties: Dendra2 (a green-to-red irreversibly photoconverting fluorescent protein with an HYG chromophore; Adam

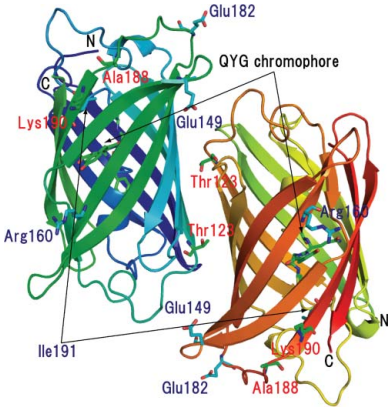

et al., 2009), Dronpa (a bright-and-dark reversibly photoswitchable fluorescent protein with a QYG chromophore; Andresen *et al.*, 2007; Stiel *et al.*, 2007), KikG (a tetrameric green-emitting fluorescent protein with a DYG chromophore; Tsutsui *et al.*, 2005) and Kaede (another green-to-red irreversibly photoconverting fluorescent protein with an HYG chromophore; Hayashi *et al.*, 2007) as well as avGFP (Ormö *et al.*, 1996). Our structural comparison revealed that the chromophore formed by Gln62-Tyr63-Gly64 (QYG) and the fixing of the conformation of the imidazole ring of His193 by hydrogen bonds and van der Waals contacts involving His193, Arg66, and Thr69 are likely to be required for the stable green emission of mAG.

2. Materials and methods

2.1. Structure solution and refinement of mAG

Expression, purification, crystallization and X-ray diffraction data collection were performed as reported previously (Ebisawa *et al.*, 2009). All of the programs used for structure determination and refinement are included in the *CCP*4 suite (Collaborative Computational Project, Number 4, 1994). Molecular replacement was carried out with the program *MOLREP* (Vagin & Teplyakov, 2000) using the coordinates of Dendra2 (76% sequence identity; PDB code 2vzx; Adam *et al.*, 2009) as the search model. The structure was built and refined using *ARP/wARP* (Lamzin & Wilson, 1993), *REFMAC*5 (Murshudov *et al.*, 1997) and *Coot* (Emsley & Cowtan, 2004). The stereochemistry of the structure was checked using the programs *PROCHECK* (Laskowski *et al.*, 1993) and *MolProbity* (Davis *et al.*, 2007). The coordinates and structure factors have been deposited in the Protein Data Bank under PDB code 3adf.

2.2. Computations

The molecular surface areas and protein–protein interface of mAG were calculated using the *PISA* server (Krissinel & Henrick, 2005). The sequence-similarity search against the PDB was performed using

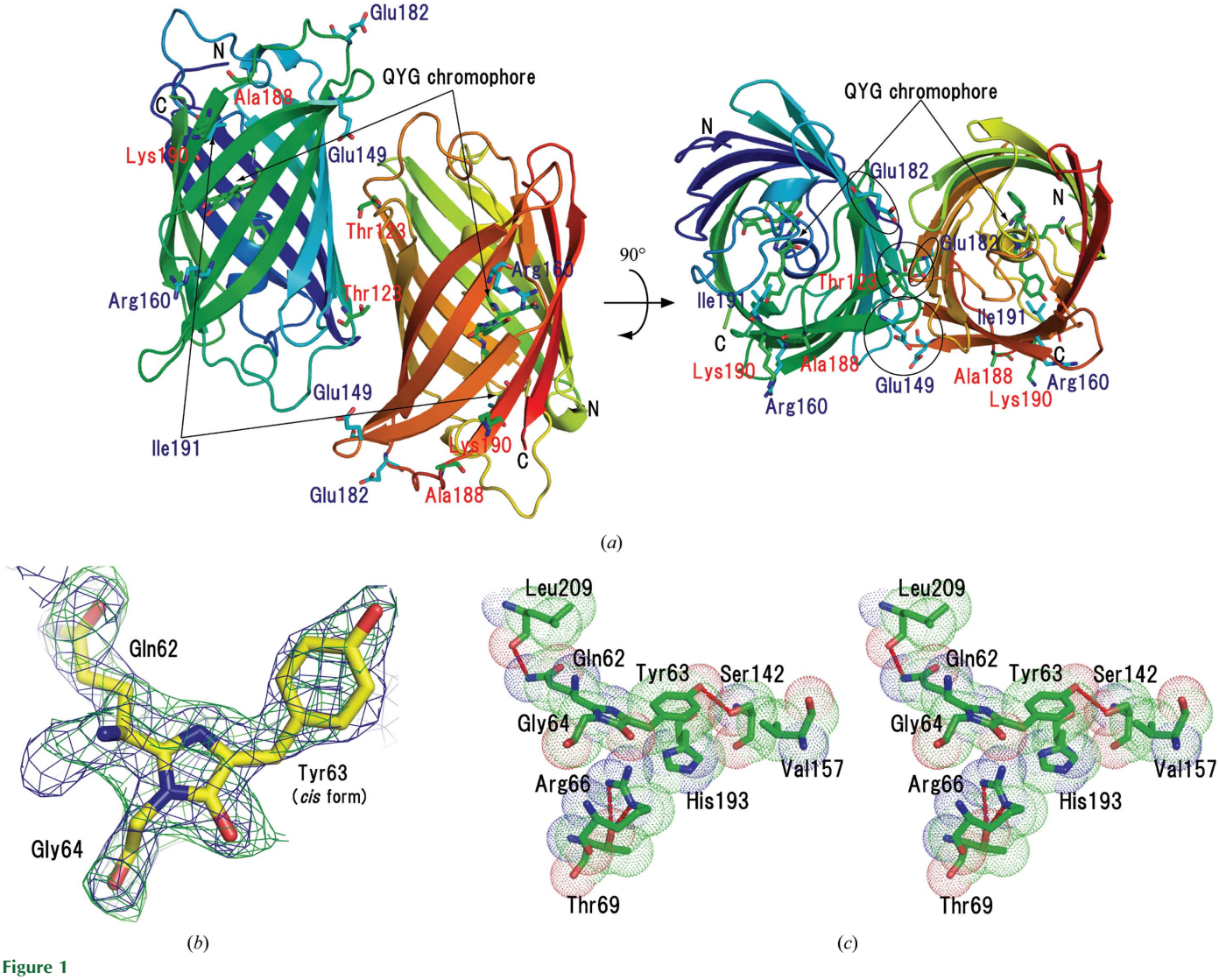

Figure 1
(*a*) Side (left) and top (right) views of the overall structure of the dimeric mAG in the asymmetric unit. The N- and C-termini are labelled N and C, respectively. The QYG chromophore (labelled in black), the residues mutated to produce mAG (Thr123, Ala188 and Lys190; labelled in red) and the additionally mutated residues (Glu149, Arg160, Glu182 and Ile191; labelled in blue) are shown as stick models. (*b*) $2F_o - F_c$ map (blue) and $F_o - F_c$ OMIT map (green) of the QYG chromophore contoured at 1σ and 2σ, respectively. (*c*) Stereoview of the QYG chromophore and nearby residues in mAG. Each van der Waals radius is shown by dots. Throughout this figure, each residue is labelled in black and hydrogen bonds are shown by red dotted lines.

Table 1
Summary of the refinement statistics.

Resolution range used for refinement (Å)	20.0–2.2
R factor† (%)	20.5
R_{free}† (%)	25.9
No. of reflections used for refinement‡	19620
Protein residues modelled	425 of 450
No. of protein atoms modelled	3454
No. of water molecules modelled	115
Mean overall *B* value (Å^2)	25.7
R.m.s.d. bond angles (°)	1.625
R.m.s.d. bond lengths (Å)	0.013
Ramachandran plot	
Residues in favoured regions (%)	96.14
Residues in allowed regions (%)	3.86
Residues in disallowed regions (%)	0

† R factor = $\sum_{hkl} ||F_{obs}| - |F_{calc}|| / \sum_{hkl} |F_{obs}|$. R_{free} was calculated using 5% of data that were excluded from refinement. ‡ This number corresponds to 95% of the number of unique reflections (20 674; Ebisawa *et al.*, 2009).

BLAST (Altschul *et al.*, 1990). Surface electrostatic potentials were calculated with *APBS* (Baker *et al.*, 2001). The structures of mAG and its homologues were superposed and the r.m.s.d. values were calculated with *DaliLite* (Holm & Park, 2000). All molecular graphics were prepared using *PyMOL* (DeLano, 2002).

3. Results and discussion

3.1. Structure determination

The crystal structure of mAG was determined at 2.2 Å resolution by the molecular-replacement method. The final structure included two mAG molecules (referred to as chains *A* and *B*) and 115 water molecules in the asymmetric unit (Fig. 1*a*). Residues 4–216 and 5–216 of chains *A* and *B*, respectively, were modelled of the 225 residues in each chain. No electron density was observed for the remaining N- and C-terminal residues. Refinement statistics are summarized in Table 1. The mAG protomer contains 12 β-strands, one α-helix and one 3_{10}-helix. It forms a β-barrel similar to other GFP-like fluorescent proteins and a coaxial central α-helix holding a Gln62-Tyr63-Gly64 (QYG) chromophore (Figs. 1*b* and 1*c*).

The buried surface area between the two mAG molecules in the asymmetric unit is 1970 Å^2, which corresponds to 11% of the total surface area of mAG and indicates that mAG is dimeric in the crystal. As mAG has been reported to be monomeric in solution, it can be inferred that the highly concentrated conditions in the crystal cause mAG to form a dimer. Karasawa *et al.* (2003) introduced three point mutations (Y123T, Y188A and F190K) to produce the monomeric mutant mAG from tetrameric AG. Among these mutated residues, Thr123 is located at the interface of the dimer and does not interact with the neighbouring protomer owing to its small size (Fig. 1*a*), whereas Tyr123 in wild-type AG is presumed to be large enough to interact with the neighbouring protomer. The other two mutated residues, Ala188 and Lys190, are located far from the dimeric interface in the crystal and thus may contribute to destabilizing the other mode of dimerization in the tetrameric assembly of AG (Fig. 1*a*).

Four additional amino-acid substitutions (R149E, A160R, D182E and V191I) were found in mAG (Ebisawa *et al.*, 2009) and the locations of these residues are distant from the QYG chromophore, suggesting that they do not affect the luminescent properties of mAG. Among these four additional amino-acid substitutions, the side chains of Glu182 and Ile191 do not face the probable tetrameric interfaces suggested from the locations of the three point mutations introduced to produce mAG. On the other hand, the R149E and A160R substitutions occur on the same side of the molecular surface as F190K, suggesting that these substitutions could take part in the establishment of mAG.

Table 2
The properties of fluorescent proteins structurally similar to mAG.

Protein	Sequence identity to mAG (%)	Chromophore	Fluorescent property	PDB code	R.m.s.d. (Å)
Dendra2	76	HYG	Green to red (irreversible)	2vzx	0.5
Dronpa	74	CYG	Green (reversibly switchable)	2iov (on-state) 2pox (off-state)	0.4 0.4
KikG	74	DYG	Green	1xss	0.6
KikGR†	74	HYG	Green to red (irreversible)	—	—
Kaede	69	HYG	Green to red (irreversible)	2gw3 (green state) 2gw4 (red state)	0.5 0.5
avGFP	27	GYG	Green	1ema	1.8

† KikGR is a variant of KikG with eight point mutations, including D62H, that confer irreversible green-to-red photoconvertibility (Tsutsui *et al.*, 2005).

3.2. The structural basis of the stable green emission of mAG

BLAST was used to search the PDB for proteins structurally similar to mAG. mAG is highly homologous to Dendra2 (Adam *et al.*, 2009), Dronpa (on-state, Andresen *et al.*, 2007; off-state, Stiel *et al.*, 2007), KikG (Tsutsui *et al.*, 2005) and Kaede (Hayashi *et al.*, 2007). Their fluorescent properties, sequence identities, PDB codes, chromophores and r.m.s.d. values with mAG are summarized in Table 2.

The irreversible green-to-red photoconversion of Dendra2, KikGR and Kaede, all of which possess the HYG chromophore, is induced by the cleavage of the peptide bond before His62 by its protonated imidazole, as indicated by the crystal structures of the green and red states of Kaede (Fig. 2*b*; PDB codes 2gw3 and 2gw4, respectively; Hayashi *et al.*, 2007). Thus, the stable green emission of mAG and KikG can be explained in part by their QYG and DYG chromophores, respectively, which lack His62.

The reversibly switchable fluorescence of Dronpa is derived from *cis* (on-state)–*trans* (off-state) isomerization at Tyr63 of the CYG chromophore accompanied by structural rearrangement of nearby amino-acid residues, including Arg66 and His193 (Fig. 2*a*; Andresen *et al.*, 2007). Interestingly, the residues forming the chromophore cavity (Arg66, Ser142, Val157 and His193) are completely conserved between Dronpa and mAG. The chromophore cavities of Dronpa in the on-state and mAG have very similar shapes which prefer the *cis* isomer of Tyr63, whereas that of Dronpa in the off-state has a unique shape which prefers the *trans* isomer of Tyr63 (Fig. 2*a*). In mAG, hydrogen bonds between the side chains of Thr69 and Arg66 fix the side-chain position of Arg66. As a result, the side-chain position of His193 is fixed by a van der Waals contact with Arg66 (Figs. 1*c* and 2*b*). Moreover, π–π stacking of the His193 and Tyr63 aromatic rings fixes the position and orientation of these rings (Fig. 1*c*). On the other hand, the side chain of Gln62 in the QYG chromophore of mAG is almost fully packed in the chromophore cavity (Fig. 2*a*). Furthermore, the side chain of Gln62 (or more accurately its $N^{\varepsilon 2}$ atom) forms a hydrogen bond to the nearby residue forming the cavity, Leu209 (main-chain O atom; Fig. 1*c*). Therefore, the QYG chromophore and nearby residues in mAG can adopt only one conformation, which fits the *cis* isomer of Tyr63 (Fig. 2*a*). In contrast, Dronpa lacks the hydrogen-bond-forming residue at position 69 (Fig. 2*b*; Ala in Dronpa *versus* Thr in mAG). Thus, the side chains of Arg66 and His193 in Dronpa are not fixed by hydrogen bonds or van der Waals contacts (Fig. 2*b*) and can therefore adopt two different conformations (Fig. 2*a*), resulting in the two different shapes of the chromophore cavity (Fig. 2*a*). In addition, the side chain of Cys62 in the CYG

chromophore of Dronpa is not fully packed in the chromophore cavity as it is shorter and less bulky than that of Gln62 in mAG, making the CYG chromophore of Dronpa more flexible in position and conformation than the QYG chromophore of mAG. As a result, the CYG chromophore of Dronpa can undergo *cis–trans* isomerization of its Tyr63 moiety, whereas the QYG chromophore of mAG can only adopt one state because the movement and conformational change of the QYG chromophore is largely restricted in mAG. In short, the different fluorescent properties of mAG and Dronpa are a result of the different amino-acid residues at positions 62 and 69: Gln *versus* Cys and Thr *versus* Ala, respectively.

The stably green-emitting protein avGFP, which has 27% sequence identity to mAG, also possesses a different mechanism of stabilizing the *cis* form of the Tyr moiety of the SYG chromophore by the steric hindrance caused by the side chain of Phe165 (Fig. 2*b*). Therefore, the stabilization of the *cis* form of the Tyr moiety in the chromophore is a common characteristic of the stable green emission of mAG, KikG and avGFP.

4. Conclusion

We have determined the 2.2 Å crystal structure of mAG and propose that the QYG chromophore (as opposed to an HYG or CYG chromophore) and the fixation of the side-chain conformations of Arg66 and His193 by hydrogen bonds and van der Waals contacts involving His193, Arg66 and Thr69 are likely to be required for stable green

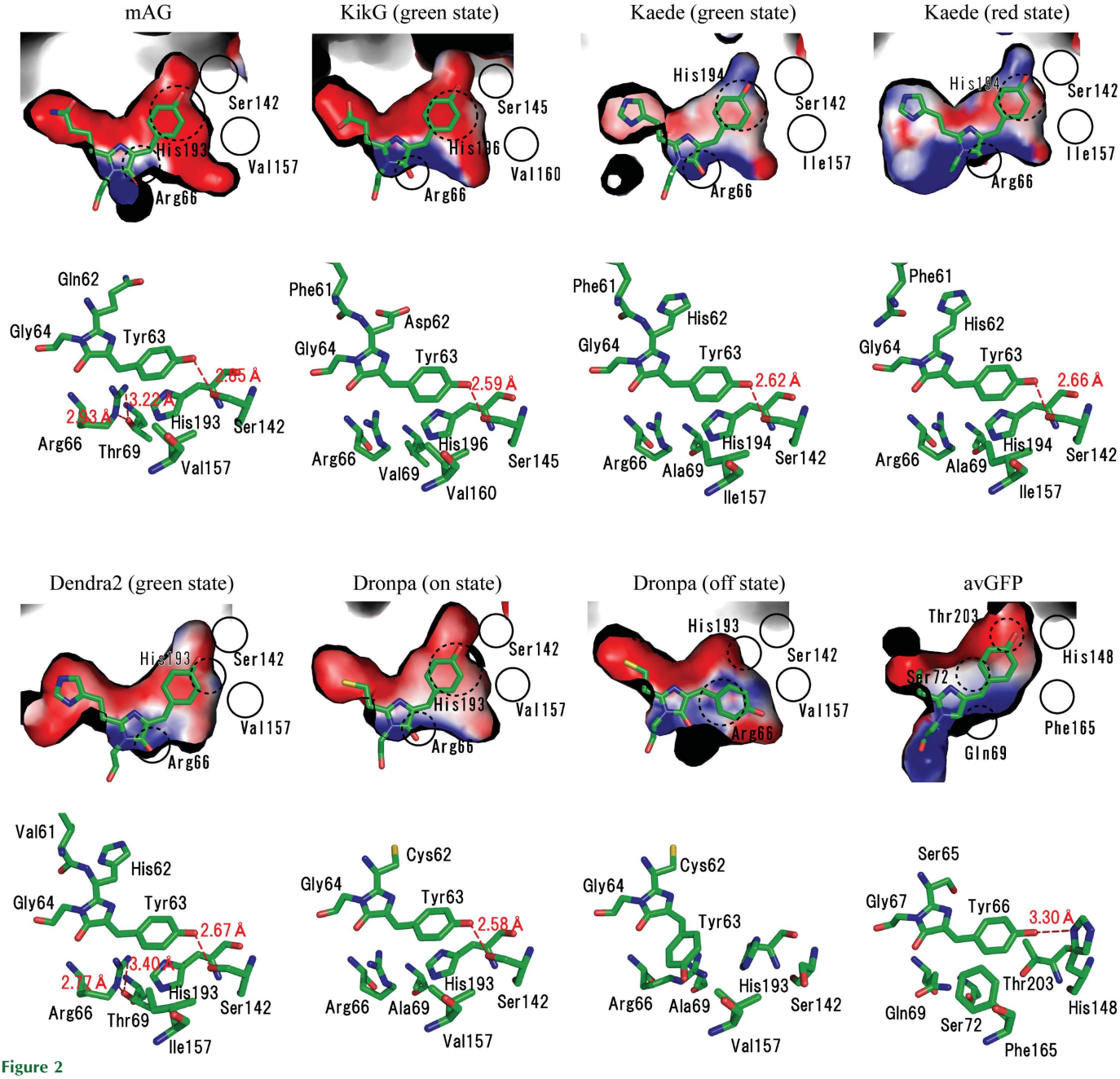

Figure 2
Electrostatic surface presentations of the chromophore cavities (upper row) and stick models of the chromophore and nearby residues (lower row) of mAG, KikG (PDB code 1xss), green-state Kaede (PDB code 2gw3), red-state Kaede (PDB code 2gw4), green-state Dendra2 (PDB code 2vzx), on-state Dronpa (PDB code 2iov), off-state Dronpa (PDB code 2pox) and avGFP (PDB code 1gfl). The electrostatic potentials are indicated as colour gradients from red ($-15k_BT$) to blue ($15k_BT$).

emission by mAG. The crystal structure of mAG will contribute to structure-based mutagenic studies to develop more useful mAG mutants with new colours, improved fluorescence and other preferable properties.

Synchrotron-radiation experiments were performed on beamline AR-NW12A at Photon Factory (Tsukuba, Japan) with the approval of the Japan Synchrotron Radiation Research Institute (Proposal No. 2008S2-001). This work was supported by the Targeted Proteins Research Program (TPRP) of the Ministry of Education, Culture, Sports, Science and Technology of Japan.

References

Adam, V., Nienhaus, K., Bourgeois, D. & Nienhaus, G. U. (2009). *Biochemistry*, **48**, 4905–4915.
Altschul, S. F., Gish, W., Miller, W., Myers, E. W. & Lipman, D. J. (1990). *J. Mol. Biol.* **215**, 403–410.
Andresen, M., Stiel, A. C., Trowitzsch, S., Weber, G., Eggeling, C., Wahl, M. C., Hell, S. W. & Jakobs, S. (2007). *Proc. Natl Acad. Sci. USA*, **104**, 13005–13009.
Baker, N. A., Sept, D., Joseph, S., Holst, M. J. & McCammon, J. A. (2001). *Proc. Natl Acad. Sci. USA*, **98**, 10037–10041.
Collaborative Computational Project, Number 4 (1994). *Acta Cryst.* D**50**, 760–763.
Davis, I. W., Leaver-Fay, A., Chen, V. B., Block, J. N., Kapral, G. J., Wang, X., Murray, L. W., Arendall, W. B. III, Snoeyink, J., Richardson, J. S., Richardson, D. C. (2007). *Nucleic Acids Res.* **35**, W375–W383.
DeLano, W. L. (2002). *PyMOL Molecular Viewer.* http://www.pymol.org.
Ebisawa, T., Yamamura, A., Kameda, Y., Hayakawa, K., Nagata, K. & Tanokura, M. (2009). *Acta Cryst.* F**65**, 1292–1295.
Emsley, P. & Cowtan, K. (2004). *Acta Cryst.* D**60**, 2126–2132.
Hayashi, I., Mizuno, H., Tong, K. I., Furuta, T., Tanaka, F., Yoshimura, M., Miyawaki, A. & Ikura, M. (2007). *J. Mol. Biol.* **372**, 918–926.
Holm, L. & Park, J. (2000). *Bioinformatics*, **16**, 566–567.
Karasawa, S., Araki, T., Yamamoto-Hino, M. & Miyawaki, A. J. (2003). *J. Biol. Chem.* **278**, 34167–34171.
Krissinel, E. & Henrick, K. (2005). *CompLife 2005*, edited by M. R. Berthold, R. Glen, K. Diederichs, O. Kohlbacher & I. Fischer, pp. 163–174. Berlin: Springer-Verlag.
Lamzin, V. S. & Wilson, K. S. (1993). *Acta Cryst.* D**49**, 129–147.
Laskowski, R. A., MacArthur, M. W., Moss, D. S. & Thornton, J. M. (1993). *J. Appl. Cryst.* **26**, 283–291.
Müller-Taubenberger, A. & Anderson, K. I. (2007). *Appl. Microbiol. Biotechnol.* **77**, 1–12.
Murshudov, G. N., Vagin, A. A. & Dodson, E. J. (1997). *Acta Cryst.* D**53**, 240–255.
Ormö, M., Cubitt, A. B., Kallio, K., Gross, L. A., Tsien, R. Y. & Remington, S. J. (1996). *Science*, **273**, 1392–1395.
Shaner, N. C., Patterson, G. H. & Davidson, M. W. (2007). *Phytopathology*, **97**, 1608–1624.
Shimomura, O. (2006). *Methods Biochem. Anal.* **47**, 1–13.
Stiel, A. C., Trowitzsch, S., Weber, G., Andresen, M., Eggeling, C., Hell, S. W., Jakobs, S. & Wahl, M. C. (2007). *Biochem. J.* **402**, 35–42.
Tsien, R. Y. (1998). *Annu. Rev. Biochem.* **67**, 509–544.
Tsutsui, H., Karasawa, S., Shimizu, H., Nukina, N. & Miyawaki, A. (2005). *EMBO Rep.* **6**, 233–238.
Vagin, A. & Teplyakov, A. (2000). *Acta Cryst.* D**56**, 1622–1624.
Yang, F., Moss, L. G. & Phillips, G. N. Jr (1996). *Nature Biotechnol.* **14**, 1246–1251.
Zhang, J., Campbell, R. E., Ting, A. Y. & Tsien, R. Y. (2002). *Nature Rev. Mol. Cell Biol.* **3**, 906–918.